Food Bioscience 64 (2025) 105968

Contents lists available at ScienceDirect

Food Bioscience

journal homepage: www.elsevier.com/locate/fbio

Total nutritional double emulsion-based supplement enriched with low-molecular-weight oyster peptides: A promising nutritional strategy for alleviating cachexia in chemotherapy-treated *Lewis* lung cancer mice

Jinzhen Li [a], Wenhong Cao [a,b], Zhongqin Chen [a,b], Haisheng Lin [a,b], Jialong Gao [a,b], Mingtang Tan [a,b], Xiaoming Qin [a,b], Huina Zheng [a,b,*]

[a] *National Research and Development Branch Center of Shellfish Processing (Zhanjiang), Guangdong Provincial Key Laboratory of Aquatic Products Processing and Safety, College of Food Science and Technology, Guangdong Ocean University, Zhanjiang, 524088, China*
[b] *Shenzhen Institute of Guangdong Ocean University, Shenzhen, 518108, China*

ARTICLE INFO

Keywords:
Total nutritional double emulsion
Low-molecular-weight oyster peptides
Lewis lung cancer
Chemotherapy
Nutritional intervention

ABSTRACT

The risk of malnutrition in cancer patients increases with prolonged chemotherapy, leading to various physiological changes. Total nutritional supplements enriched with low-molecular-weight oyster peptides have shown potential as specialized medical interventions to improve chemotherapy-induced malnutrition. The present study evaluated the nutritional quality of total nutritional double emulsion (TNDE) and assessed its effects as a nutritional intervention in *Lewis* lung cancer (LLC) mice undergoing chemotherapy. Nutritional analysis revealed that TNDE possesses high nutritional quality, containing 45.41% essential amino acids, 41.72% hydrophobic amino acids, and 38% polyunsaturated fatty acids. *In vivo* analysis demonstrated significant weight loss, increased insulin resistance, suppressed immune function, and organ damage in chemotherapy-treated animals, indicating an elevated risk of cachexia. TNDE administration effectively mitigated chemotherapy-induced cachexia by improving body weight, reducing insulin resistance, and alleviating spleen and liver injuries compared to LLC mice undergoing chemotherapy without TNDE supplementation. TNDE also enhanced IgG and IgM levels while suppressing TNF-α and IL-6. The alleviation of cachexia in LLC mice may involve modulation of metabolic pathways, such as steroid hormone and folate biosynthesis. These findings provide a theoretical basis for developing and applying marine-derived peptide double emulsion-based, nutrient-dense formulations for cancer patients.

1. Introduction

Cancer treatment often requires costly medications and extended time commitments, imposing substantial economic burdens on patients, families, and society while posing significant challenges to global health (Wu, Luo, & Xu, 2024). According to a 2024 report by the International Agency for Research on Cancer, lung cancer remains the most commonly diagnosed cancer, with the highest incidence and mortality rates globally (Bray et al., 2024). Non-small cell lung cancer (NSCLC) accounts for approximately 85% of all lung cancer cases. A critical challenge in managing NSCLC is its frequent late diagnosis, with over 75% of cases identified at advanced stages due to inadequate early detection methods (Xiao et al., 2023). Moreover, NSCLC has traditionally been considered a radiation-resistant malignancy, often necessitating pharmaceutical chemotherapy as a primary treatment approach (Li et al., 2022). Despite its effectiveness, chemotherapy agents such as cyclophosphamide (CTX) and tyrosine kinase inhibitors often impair immune and metabolic system functions (Wang, Hsia, Wu, & Wu, 2021; Zhang, Zhou, et al., 2021). Cachexia, a severe and common complication in advanced lung cancer, arises from immunosuppression, acute malnutrition, and metabolic disturbances caused by prolonged chemotherapy (Alduais, Zhang, Fan, Chen, & Chen, 2023).

Previous studies have demonstrated that supplementation with nutrient-dense foods formulation during chemotherapy can enhance its efficacy and prevent the progression of cachexia in tumor-bearing mice (Liu et al., 2019, 2020; Wang, Hsia, et al., 2021). Adequate protein and calorie intake is crucial for effective nutritional support, making enteral nutritional interventions valuable adjunct therapies for managing

* Corresponding author. College of Food Science and Technology, Guangdong Ocean University, Zhanjiang, Guangdong Province, 524088, China.
E-mail address: zhenghn@gdou.edu.cn (H. Zheng).

https://doi.org/10.1016/j.fbio.2025.105968
Received 4 December 2024; Received in revised form 18 January 2025; Accepted 20 January 2025
Available online 21 January 2025

cachexia in oncology patients (Mele et al., 2021). Addressing overnutrition and malnutrition to promote healthy lives aligns with the United Nations Sustainable Development Goals, which recognize the importance of health for economic growth (Michel et al., 2024). Therefore, well-balanced nutritional formulations in nutrient-dense foods are essential for alleviating cachexia in cancer patients.

Nutrient-dense formulations aim to assess a product's composition, including its caloric and nutrient profile, by combining components in precise proportions to optimize sensory attributes and functionality such as appearance, flavor, and health benefits (Michel et al., 2024). Traditional emulsion-based supplements, typically oil-in-water (O/W) emulsions, contain high levels of proteins, oils, carbohydrates, and micronutrients (Li et al., 2023). However, their oil-in-water structure limits the incorporation of certain water-soluble active ingredients, particularly those with unpleasant odors. Double emulsions ($W_1/O/W_2$) have emerged as a promising alternative, enabling efficient encapsulation of active components such as peptides, vitamins, and polyunsaturated fatty acids while reducing calorie content by partially substituting lipids with water (Kumar et al., 2022). However, double emulsions exhibit thermodynamic instabilities, including phase separation, foaming, and flocculation, compromising product stability and quality, thereby hindering their practical application in the nutritional beverage market. The complex composition of emulsion-based nutritional beverages, involving diverse substances such as water and oils, increases their susceptibility to variations during manufacturing and storage, further challenging their stability, quality, and shelf life (Drapala, Mulvihill, & O'Mahony, 2018). Although double emulsions are inherently less stable than traditional emulsions, their broader applications in functional foods, including encapsulating peptides and dietary lipids and producing low-energy products with enhanced sensory attributes, make them valuable in the food industry (Buyukkestelli & El, 2019, 2021; Lamba, Sathish, & Sabikhi, 2015; Ying et al., 2021). Consequently, the stabilization of double emulsions has become a focal point of research to overcome these challenges.

Previous studies have shown that combining high-speed shear with ultrasonic treatment enhances the thermodynamic stability of double emulsion nutritional supplements fortified with low-molecular-weight oyster peptides (LOPs), particularly by improving phase stability (Li et al., 2023). Moreover, ultrasound-treated total nutritional double emulsion (TNDE) demonstrated superior wettability, freeze-thaw stability, long-term retention of fat-soluble nutrients, and favorable sensory attributes (Li et al., 2024). TNDE is a comprehensive nutritional formula incorporating marine-derived peptides, fish oil (rich in eicosapentaenoic acid and docosahexaenoic acid), vitamins, and other micronutrients. As a marine-derived protein, LOPs have been shown to mitigate chemotherapy-induced immunosuppression in *Lewis* lung cancer (LLC) mice by modulating the gut microbiota, potentially enhancing immune function (Li et al., 2022). Additionally, substantial evidence indicates that ω-3 polyunsaturated fatty acids (PUFAs) can partially inhibit inflammation through interactions with the cell surface and intracellular receptors involved in inflammatory signaling and gene expression regulation (Calder, 2015). Therefore, TNDE represents a viable strategy for enteral nutritional support during chemotherapy in cancer patients. However, limited research exists on the nutritional and biological efficacy of double emulsion-based enteral nutrition beverages, highlighting the need for further investigation.

This study aims to investigate the nutritional quality and cachexia-ameliorating effects of TNDE. Nutritional properties were analyzed through amino acid and fatty acid profiling. Growth parameters, insulin resistance, cytokine levels, hematological indices, and organ damage were assessed in chemotherapy-induced LLC mice. Untargeted liver metabolomics was also utilized to elucidate the biological mechanisms underlying the effectiveness of TNDE as a nutritional intervention.

2. Materials and methods

2.1. Materials and chemicals

The TNDE, a double emulsion system, was prepared following a methodology previously described (Li et al., 2024). The W_1/O emulsion was prepared using a high-speed homogenizer (IKA T18 digital, Ultra-Turrax, Staufen, Germany) at 13,000 rpm for 2 min. The W_1/O emulsion was then gradually incorporated into the W_2-phase phase and homogenized at 7000 rpm for 2 min. Subsequently, the TNDE was subjected to sonication (20 kHz, Sonifier 250D, Branson Ultrasonics Co., Ltd., Shanghai, China) for 5 min at 100 W, with 4-s on-cycles and 2-s off-cycles. Finally, the TNDE was pasteurized for subsequent nutritional quality and *in vivo* nutrient support evaluations. Finally, the pasteurized samples were stored for a maximum of 72 h to assess the nutritional quality. In contrast, the *in vivo* nutrient support evaluation of TNDE was conducted using freshly prepared with pasteurized samples.

CTX was purchased from Sigma-Aldrich (St. Louis, MO, USA). Enzyme-linked immunosorbent assay (ELISA) kits for insulin, IgG, IgM, TNF-α, and IL-6 were sourced from Meimian Industrial Co., Ltd. (Yancheng, China). The LLC cells used in the present study were sourced from the Chinese Academy of Sciences (Shanghai, China). All other reagents were of analytical grade, and ultra-pure MilliQ water was employed in all experimental procedures.

2.2. Nutritional characterization of TNDE

The total content of raw proteins, lipids, carbohydrates, and dietary fiber in TNDE were determined using standard methods (International, 2023). The profiles of amino acids and fatty acids in TNDE were examined according to the protocol described by Hashemirad, Behfar, and Kavoosi (2024), with slight adjustments. In brief, TNDE underwent hydrolysis at 110 °C in 6 M HCl for 24 h, followed by a cooling phase. Afterward, the undigested substances were separated through centrifugation at 3000*g* for 10 min. The resulting suspension of amino acids was then dried, reconstituted in a 500 mM NaCl solution (10 mg/mL), and analyzed using an automatic amino acid analyzer (Model L-8900, Hitachi Ltd., Tokyo, Japan). To determine the fatty acid composition, the lipids from TNDE were extracted using the Folch method (chloroform: methanol: water = 2:1:0.8, v/v/v). The lipid extract (1:10 v/v) was then combined with a methanol-sulfuric acid (80:20 v/v) mixture to form fatty acid methyl esters, which were incubated at 80 °C for 120 min. The fatty acid methyl esters were subsequently extracted with hexane using centrifugation at 3000*g* for 10 min, and the resulting profiles were analyzed using an Agilent gas chromatograph (Agilent 7890A GC, Agilent Technologies Inc., California, USA).

Three nutritional parameters were assessed using the amino acid composition of TNDE, as outlined in earlier studies (Mir, Riar, & Singh, 2019). There calculation formulas are shown in Eqs. (1)–(5).

(a) Protein efficiency ratio (PER)

$$PER_1 = \text{-}0.684 + 0.456 \times Leu \text{ - } 0.047 \times Pro \tag{1}$$

$$PER_2 = \text{-}0.468 + 0.454 \times Leu \text{ - } 0.105 \times Tyr \tag{2}$$

$$PER_3 = \text{-}1.816 + 0.435 \times Met + 0.78 \times Leu + 0.211 \times His \text{ - } 0.944 \times Tyr \tag{3}$$

(b) Essential amino acid index (EAAI)

$$EAAI = \sqrt{\frac{Lys_a \times Thr_a \times \cdots \times His_a}{Lys_b \times Thr_b \times \cdots \times His_b}} \tag{4}$$

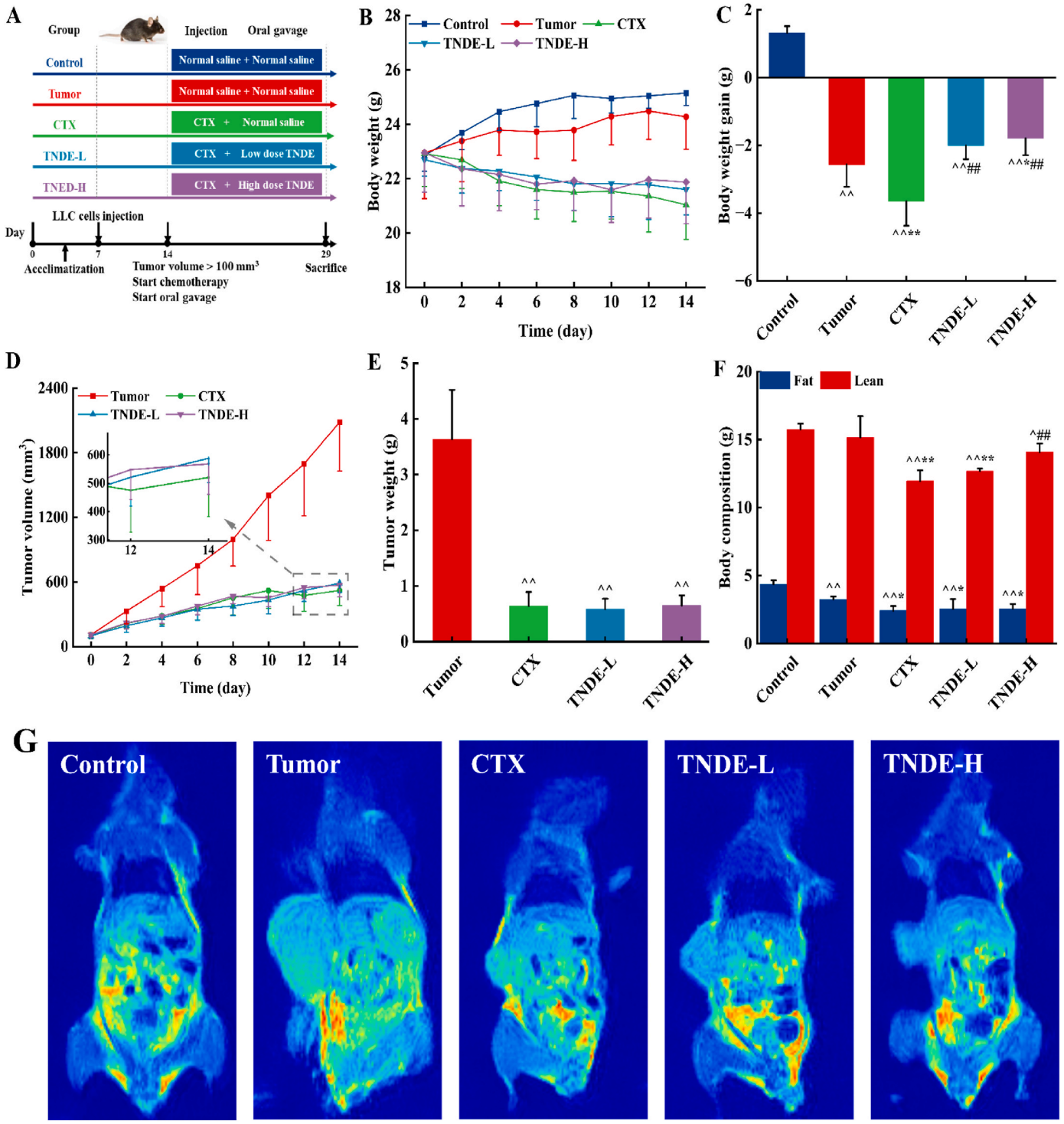

Fig. 1. The ameliorative effects of total nutrition double emulsion (TNDE) on growth of the LLC mice undergoing CTX-chemotherapy ($n = 8$). (A) Animal experimental protocol. (B) Body weight. (C) Body weight gain. (D) Tumor volume. (E) Tumor weight. (F) Lean and fat mass. (G) Representative photographs of adipose distribution. $^{\wedge}P < 0.05$, $^{\wedge\wedge}P < 0.01$ versus control group; $^{*}P < 0.05$, $^{**}P < 0.01$ versus tumor group; $^{\#}P < 0.05$, $^{\#\#}P < 0.01$ versus CTX group.

in this context, *a* represents the amino acids of TNDE, and *b* signifies the amino acids of standard protein.

(c) Biological value (BV)

$$BV = 1.09 \times EAAI - 11.7 \quad (5)$$

2.3. Animals experimental design

Male specific pathogen-free C57BL/6J (6-week-old) were purchased form BesTest Bio-Tech Co., Ltd (Zhuhai, China). All animal procedures were approved by the Animal Ethics Committee of Guangdong Ocean University (protocol number GDOU-LAE-2022-016). As illustrated in Fig. 1A, each six-week-old male C57BL/6J mouse was injected with 1×10^6 LLC cells (at 1×10^7 cells/mL) into the right flank. Mice were then

randomly assigned to five groups, each consisting of eight mice: the control group (no LLC cells), the tumor group, the CTX group (60 mg/kg), the CTX combined with low-dose TNDE group (TNDE-L, 0.4 mL/d), and the CTX combined with high-dose TNDE group (TNDE-H, 0.8 mL/d). Dosage levels were determined based on previous studies with minor adjustments (Wang, Hsia, et al., 2021).

CTX chemotherapy was administered to all groups, except the control and tumor groups, for two weeks once tumor volume reached approximately 100 mm^3. Mice in the TNDE groups received daily oral administration of TNDE, while other groups received saline via oral gavage. Body weight and tumor growth were monitored regularly during the two-week treatment period. After completing the nutritional intervention, mice were fasted for 12 h, anesthetized using CO_2 ether asphyxiation, and euthanized via cervical dislocation. Blood samples were collected through orbital bleeding, and liver tissues were harvested and stored at −80 °C for subsequent analysis.

2.4. Analysis of body composition

Body composition, including lean and fat mass distribution, was analyzed for each mouse using magnetic resonance imaging (MRI) equipment (Miumag Analytical Instrument Co., Ltd, Suzhou, China). Mice were first weighed and placed directly into a 60 mm diameter cylinder for scanning. Each mouse was scanned for approximately 2 min to collect overall body composition data. Adipose tissue distribution was further assessed while mice were maintained under anesthesia with 2% isoflurane for positioning, followed by a 10-min imaging session (Yang et al., 2022).

2.5. Analysis of insulin resistance

Fasting blood glucose (FBG) was measured using a commercial glucometer (Yuyue Medical Device Company, Shanghai, China) with blood collected from the tail. For the oral glucose tolerance test (OGTT), mice were fasted for 12 h and then administered a glucose solution via oral gavage at 2 g/kg. Blood glucose levels were recorded at 0-, 15-, 30-, 60-, 90-, and 120-min post-gavage. Additionally, serum insulin levels were measured using an ELISA kit. The area under the curve (AUC) for glucose tolerance was calculated, and statistical analyses were performed using OriginPro 2022 (OriginLab Corporation Inc., USA).

2.6. Analysis of immunity indicators

Blood samples were collected via orbital puncture after euthanasia and centrifuged at 1200 g for 20 min at 4 °C to isolate serum. The IgG, IgM, TNF-α, and IL-6 levels were quantified using an ELISA kit according to the manufacturer's guidelines.

2.7. Analysis of hematologic parameters

During euthanasia, 0.2 mL of blood was collected and analyzed for hematological parameters using a whole-cell autoanalyzer (BC-2800vet, Mindray Animal Medical Co., Ltd., Shenzhen, China).

2.8. Histological analysis of the spleen and liver

The spleen and liver were preserved in 4% (v/v) paraformaldehyde for one day. Fixed tissues were embedded in paraffin, sectioned into 5 μm slices, stained with hematoxylin and eosin (H&E), and dehydrated for sealing. Pathological changes in these tissues were examined under an optical microscope, and images were captured for analysis.

2.9. Analysis of liver UHPLC-QE-MS non-target metabolomics

Fifty milligrams of liver tissue were precisely weighed, and metabolites were extracted using 400 μL of a methanol-water solution (4:1, v/v). The samples were incubated at −20 °C, homogenized for 6 min at 50 Hz using a high-throughput tissue crusher, vortexed for 30 s, and ultrasonicated at 40 kHz for 30 min at 5 °C. Following sonication, the samples were kept at −20 °C for 30 min to precipitate proteins. The supernatant was then separated by centrifugation at 13,000 g for 15 min at 4 °C and gently transferred into vials for LC-MS/MS analysis. A pooled quality control (QC) sample was prepared to ensure analytical stability and consistency by combining aliquots from all experimental samples. These QC samples were processed and analyzed identically to the experimental samples to assess system reliability.

Metabolites were separated using an ultra-high-performance liquid chromatography (UHPLC) system with a C18 column (100 mm × 2.1 mm i.d., 1.7 μm). The injection volume was 2 μL, with a flow rate of 0.4 mL/min, and the column temperature was maintained at 40 °C. MS data acquisition was performed using a UHPLC-QE-MS system with an electrospray ionization source operating in positive and negative ionization modes. Optimized settings included an auxiliary gas warmer at 40 °C, a sheath gas flow rate of 40 psi, an auxiliary gas flow rate of 30 psi, and ion spray voltages of −2800 V in negative mode and 3500 V in positive mode. MS/MS data were acquired using a normalized collision energy of 20, 40, and 60 V. Measurements were performed using the data-dependent acquisition method, with a detection range of 70–1050 m/z.

Table 1
The nutritional profiles of TNDE.

Parameter	TNDE
Total calories (Kcal/100 g)	177.34
Total fat (g/100 g)	9.35
Total carbohydrate (g/100 g)	11.76
Protein (g/100 g)	8.76
Dietary fiber (g/100 g)	4.80
PER_1	4.15
PER_2	4.54
PER_3	7.19
Biological value (%)	78.98
Essential amino acid index	83.19

2.10. Statistical analysis

Statistical analyses were conducted using one-way analysis of variance (ANOVA) in SPSS version 26 (IBM, USA). Post-hoc comparisons were performed using the least significant difference (LSD) method to evaluate group differences. Metabolites were identified and annotated using the HMDB 4.0 and KEGG databases. Differential metabolites were determined based on criteria of VIP >1 and $P < 0.05$. KEGG pathway analysis was performed on these metabolites to explore potential metabolic pathways. The P-value <0.05 was recognized as statistical significance.

3. Results and discussion

3.1. Nutritional characterization of TNDE

3.1.1. Nutritional profile of TNDE

TNDE is an emulsion-based nutritional product enriched with protein, energy, LOPs, multivitamins, and multiminerals. Nutritional parameters were determined based on its amino acid profile (Table 1). Protein Efficiency Ratio (PER) was used to evaluate protein quality, where values below 1.5 indicate poor quality and values above 2 indicate high-quality protein (Vinayashree & Vasu, 2021). Biological Value (BV), which assesses the proportion of dietary protein assimilated into human proteins, typically ranges from 70% to 100% for high-quality proteins (Mir et al., 2019). TNDE demonstrated a BV of 78.98%, confirming its superior nutritional quality. Furthermore, the Essential Amino Acid Index (EAAI) of TNDE was comparable to that of most oral nutritional supplements (Liu et al., 2020).

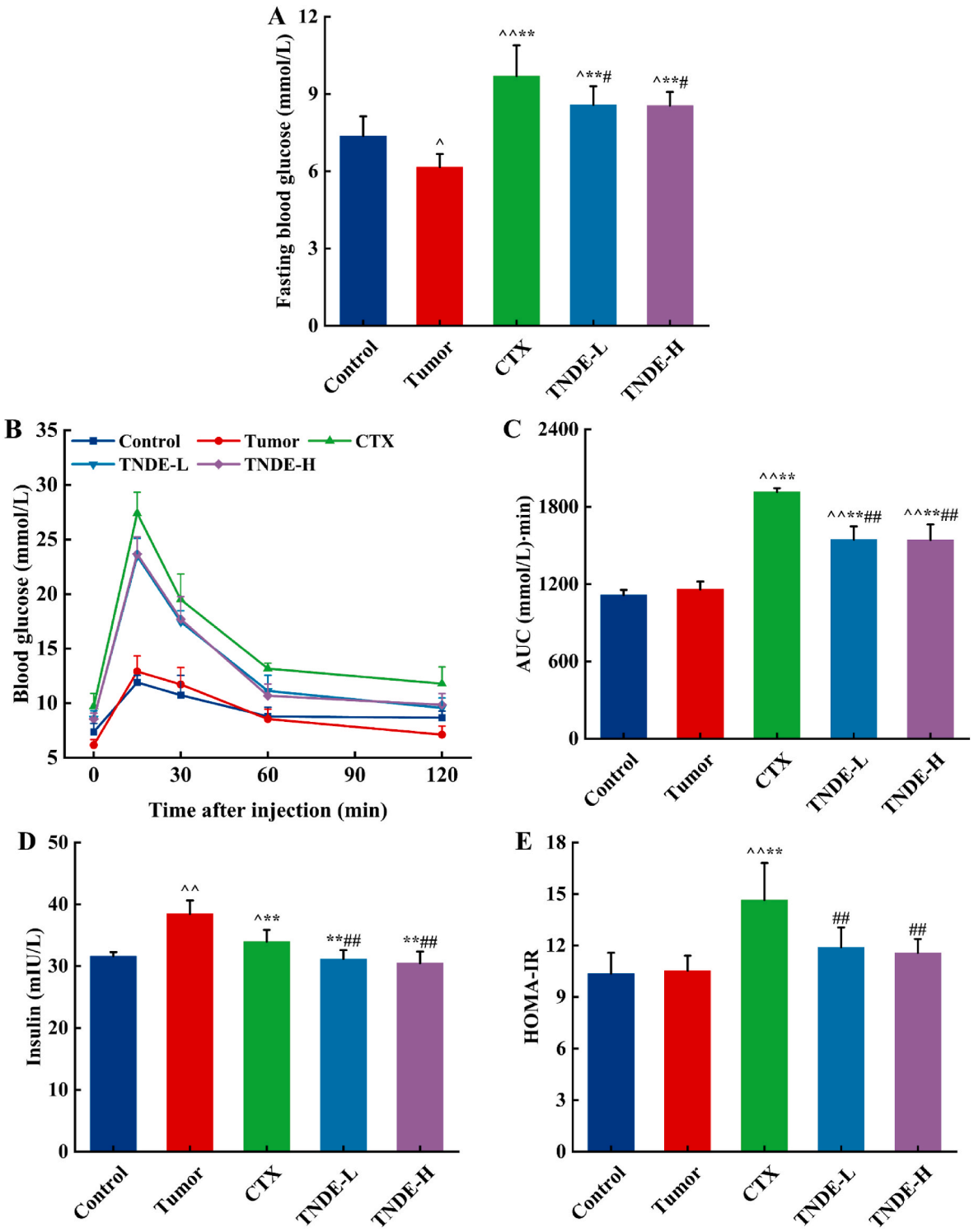

Fig. 2. The ameliorative effects of TNDE on insulin resistance in LLC mice undergoing CTX-chemotherapy. (A) Fasting blood glucose measured after fasting for 12 h ($n = 8$). (B) Oral glucose tolerance test (OGTT) upon 12 h fasting. (C) Area under curve (AUC) of the OGTT. (D) Insulin in blood. (E) Homeostatic model assessment for insulin resistance (HOMA-IR). $^{\wedge}P < 0.05$, $^{\wedge\wedge}P < 0.01$ versus control group; $^{*}P < 0.05$, $^{**}P < 0.01$ versus tumor group; $^{\#}P < 0.05$, $^{\#\#}P < 0.01$ versus CTX group.

3.1.2. *Amino acid profile of TNDE*

The nutritional value of TNDE is largely determined by its amino acid composition, as detailed in Table S1. The analysis indicated that TNDE is a rich source of essential amino acids, comprising approximately 45.41% of the total amino acids (T-AAs). Notably, branched-chain amino acids (BCAAs) account for about 23.75% of the T-AAs. A diet rich in BCAAs has been shown to improve the prognosis of patients with malignant tumors by reducing mortality and complications. This benefit is primarily due to their ability to promote protein synthesis and reduce insulin resistance, thereby enhancing treatment outcomes (Nie, He, Zhang, Zhang, & Ma, 2018; Yao et al., 2023). Additionally, TNDE is abundant in hydrophobic amino acids, including methionine (Met), tyrosine (Tyr), phenylalanine (Phe), proline (Pro), isoleucine (Ile), alanine (Ala), valine (Val), and leucine (Leu), which together constitute

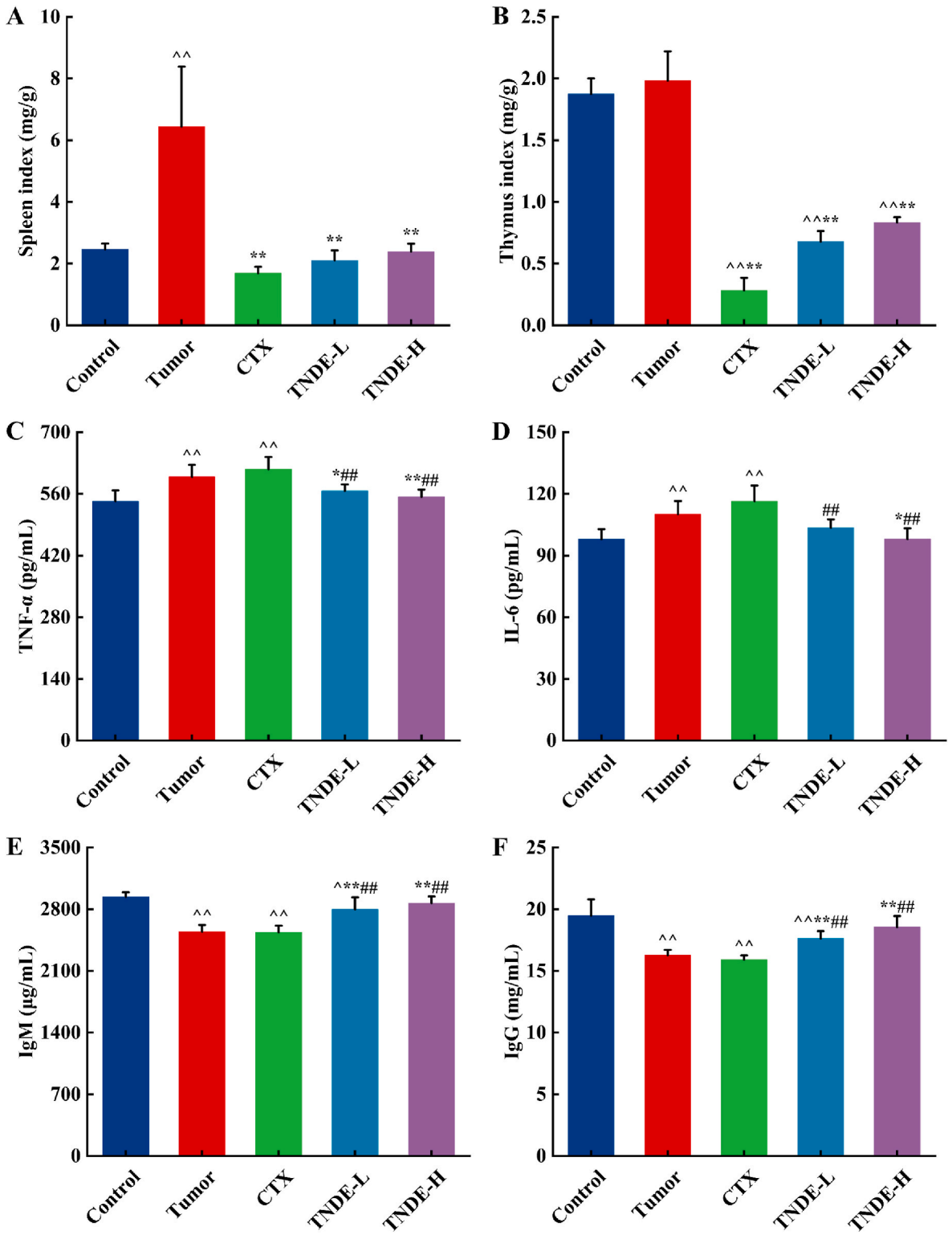

Fig. 3. The ameliorative effects of TNDE on immune organ index, serum cytokines and immunoglobulin in LLC mice undergoing CTX-chemotherapy ($n = 8$). (A) Spleen index. (B) Thymus index. (C) TNF-α levels. (D) IL-6 levels. (E) IgG levels. (F) IgM levels. $^{\wedge}P < 0.05$, $^{\wedge\wedge}P < 0.01$ versus control group; $^{*}P < 0.05$, $^{**}P < 0.01$ versus tumor group; $^{\#}P < 0.05$, $^{\#\#}P < 0.01$ versus CTX group.

approximately 41.72% of the T-AAs. These hydrophobic amino acids have demonstrated efficacy in enhancing immune regulation (Liu et al., 2023). These findings suggest that TNDE holds significant potential for improving therapeutic outcomes and modulating immune responses in patients undergoing chemotherapy.

3.1.3. *Fatty acid composition of TNDE*

The fatty acid composition of TNDE is detailed in Table S2. Unsaturated fatty acids accounted for the largest proportion of the oil phase, comprising over 57.48% of the total oil content. Notably, eicosapentaenoic acid (EPA) and docosahexaenoic acid (DHA) were present at concentrations of 4.73% and 3.24%, respectively. Foods rich in EPA and

DHA have been shown to significantly improve cardiovascular health and mitigate tumor-related complications (Cockbain, Toogood, & Hull, 2012; Freitas & Campos, 2019). The oil phase of TNDE also contains medium-chain triglycerides (MCT), contributing to its saturated fatty acid content. MCT is an ideal dietary fat for cancer patients with digestive disorders, as it can alleviate chemotherapeutic side effects, including disruptions in glucose and lipid metabolism and neuroinflammation (Augustin et al., 2018). Therefore, TNDE holds the potential to improve digestive health, enhance nutrient absorption, and provide energy support.

3.2. Nutritional interventions of TNDE

3.2.1. Effect of TNDE on growth of LLC mice

Our previous study reported that CTX inhibits cancer cell proliferation through cytotoxic effects, contributing to its anti-tumor activity (Li et al., 2022). Tumor cells exhibit a faster rate of nutrient uptake and metabolism than normal cells. However, no evidence indicates whether nutritional support diminishes chemotherapy efficacy or promotes tumor cell proliferation. To address this, the present study used LLC mice to evaluate the therapeutic effects of TNDE as a supplemental nutrition intervention. As shown in Fig. 1B and C, mice in the CTX group exhibited remarkable weight loss compared with the control and tumor groups ($P < 0.01$). Chemotherapy reduced body weight by 13.12% compared to pre-chemotherapy levels, likely due to the toxic effects of CTX on Normal cells, resulting in acute malnutrition in mice without nutritional intervention. TNDE supplementation alleviated weight loss in chemotherapy-treated mice compared to the CTX group. Tumor volume and mass were also measured to assess whether nutritional support influenced chemotherapy outcomes. Compared to the tumor group, mice undergoing chemotherapy showed significantly inhibited tumor growth ($P < 0.01$). Importantly, TNDE supplementation did not attenuate the chemotherapeutic effects (Fig. 1D and E). These findings suggest that TNDE effectively mitigates weight loss caused by chemotherapy without compromising its efficacy, likely due to the high protein quality and nutritional value of TNDE.

During tumor treatment, endogenous lipolysis accelerates due to the release of lipolytic hormones, resulting in reduced fat storage, progressive body wasting, and weight loss (Torricelli et al., 2020). To confirm the nutritional supportive effects of TNDE, body fat distribution was analyzed in LLC mice (Fig. 2F and G). Compared with normal mice and LLC mice without chemotherapy, chemotherapy significantly reduced lean body mass and abdominal adipose tissue mass ($P < 0.01$), indicating that malnutrition in chemotherapy-treated mice is associated with impaired adipose metabolism. TNDE supplementation gradually restored lean and adipose tissue mass to pre-chemotherapy levels. Subcutaneous and abdominal fat stores increased, alleviating symptoms of chemotherapy-induced weight loss. These findings demonstrate that TNDE effectively mitigates malnutrition in mice, likely due to its well-balanced dietary fat formulation.

Table 2
Effect of TNDE on hematological parameters.

Group	RBC (10^{12}/L)	HGB (g/L)	WBC (10^9/L)	GRAN (10^9/L)	LYM (10^9/L)
Control	9.1 ± 0.7	149.6 ± 10.4	4.9 ± 1.5	0.6 ± 0.2	4.2 ± 1.3
Tumor	6.9 ± 1.6$^{\hat{}}$	118.2 ± 24.9$^{\hat{}}$	9.3 ± 2.9$^{\hat{}}$	2.6 ± 1.7$^{\hat{}}$	6.1 ± 1.2$^{\hat{}}$
CTX	5.3 ± 1.3$^{\hat{}}$*	80 ± 18.6$^{\hat{}}$**	0.6 ± 0.2$^{\hat{}}$**	0.2 ± 0.1**	0.6 ± 0.1$^{\hat{}}$**
TNDE-L	6.5 ± 0.6$^{\hat{}}$	92.8 ± 6.9$^{\hat{}}$*	0.8 ± 0.3$^{\hat{}}$**	0.4 ± 0.2**	1.2 ± 0.1$^{\hat{}}$**
TNDE-H	7.2 ± 0.9$^{\hat{}\#}$	97.8 ± 14.3$^{\hat{}}$	1.2 ± 0.5$^{\hat{}}$**	0.3 ± 0.2**	1.2 ± 0.4$^{\hat{}}$**

$^{\hat{}}P < 0.05$, $^{\hat{}}P < 0.01$ versus control group; $^{*}P < 0.05$, $^{**}P < 0.01$ versus tumor group; $^{\#}P < 0.05$, $^{\#\#}P < 0.01$ versus CTX group.

3.2.2. Effect of TNDE on insulin resistance in LLC mice

Insulin resistance (IR) is closely associated with the development and progression of metabolic disorders such as diabetes, hypertension, and cancer (Godsland, 2010; Yang et al., 2022). IR disrupts glucose regulation and utilization, posing significant health risks and adversely affecting patient quality of life (Zhao et al., 2023). Previous findings indicated that TNDE alleviates chemotherapy-induced weight loss in LLC mice. Building on these results, the study aimed to evaluate whether TNDE could also mitigate chemotherapy-induced IR. As illustrated in Fig. 2, fasting blood glucose levels significantly increased in the chemotherapy group compared to non-chemotherapy mice ($P < 0.01$). Oral glucose tolerance tests revealed impaired glucose sensitivity in chemotherapy-induced LLC mice. However, fasting blood glucose levels normalized following TNDE supplementation ($P < 0.05$). Furthermore, TNDE administration significantly reduced the elevated insulin levels induced by tumor growth ($P < 0.01$). Consistently, the homeostatic model assessment for IR (HOMA-IR) was significantly higher in LLC mice that received chemotherapy compared to normal and tumor-only groups but returned to normal levels following TNDE treatment ($P < 0.01$). These results suggest that TNDE positively regulates glucose homeostasis, likely due to its marine-derived peptides, consistent with findings from previous studies (Wang et al., 2024).

3.2.3. Effect of TNDE on immunomodulation in LLC mice

The cytotoxic chemotherapy agent CTX is a non-targeted, broad-spectrum chemotherapeutic that effectively inhibits tumor cells and exerts toxic effects on normal cells, particularly immune cells (Zhang et al., 2023). Previous research has demonstrated that LOPs can attenuate CTX-induced immunosuppression (Li et al., 2022). Therefore, we investigated whether TNDE, enriched with LOPs, could exhibit similar protective effects against immunosuppression in LLC mice undergoing chemotherapy (Fig. 3A and B). Mice receiving TNDE nutritional support exhibited higher immune organ indices compared to the CTX group. Increased TNDE doses led to spleen indices gradually returning to normal levels. The spleen and thymus play essential roles in immune function, with their organ indices serving as critical markers of immunoregulatory capacity (Wang, Hsia, et al., 2021). These results indicate that TNDE can partially mitigate chemotherapy-induced immunosuppression. Spleen and thymus enlargement was observed in LLC mice not receiving chemotherapy, likely due to antigen release from proliferating tumor cells, which may induce immune organ expansion.

Pro-inflammatory cytokines, TNF-α and IL-6, are critical in the development and progression of various inflammatory diseases. Malignancies and complications arising from tumor treatment are often associated with elevated levels of these cytokines (Naudhani, Thakur, Ni, Zhang, & Wei, 2021). Compared with the control group, serum levels of the TNF-α and IL-6 were remarkably elevated in both the tumor and CTX groups (Fig. 3C and D) ($P < 0.01$). These findings indicate that tumor progression and chemotherapy stimulate the release of pro-inflammatory cytokines, thereby affecting cellular immunity and inhibiting immune regulation. Serum levels of these pro-inflammatory cytokines were significantly reduced in TNDE-supplemented mice compared with the CTX group ($P < 0.01$) and returned to levels comparable to those of normal mice. These results suggest that oral nutritional supplements enriched with prebiotic ω-3 PUFAs, such as EPA and DHA, may effectively reduce pro-inflammatory cytokine release (Zepeda-Hernández, Garcia-Amezquita, Requena, & García-Cayuela, 2021).

Malnutrition symptoms in treated tumor patients are often followed by immunosuppression, increasing susceptibility to infections (Windsor et al., 1998). As shown in Fig. 3E and F, TNDE supplementation at different oral doses resulted in a dose-dependent increase in IgG and IgM serum levels in LLC mice undergoing chemotherapy. Immunoglobulins, essential proteins for immune responses, possess antibody functions and play diverse roles in immunity. IgG, the most abundant serum immunoglobulin, and IgM, the largest in molecular weight, serve as key

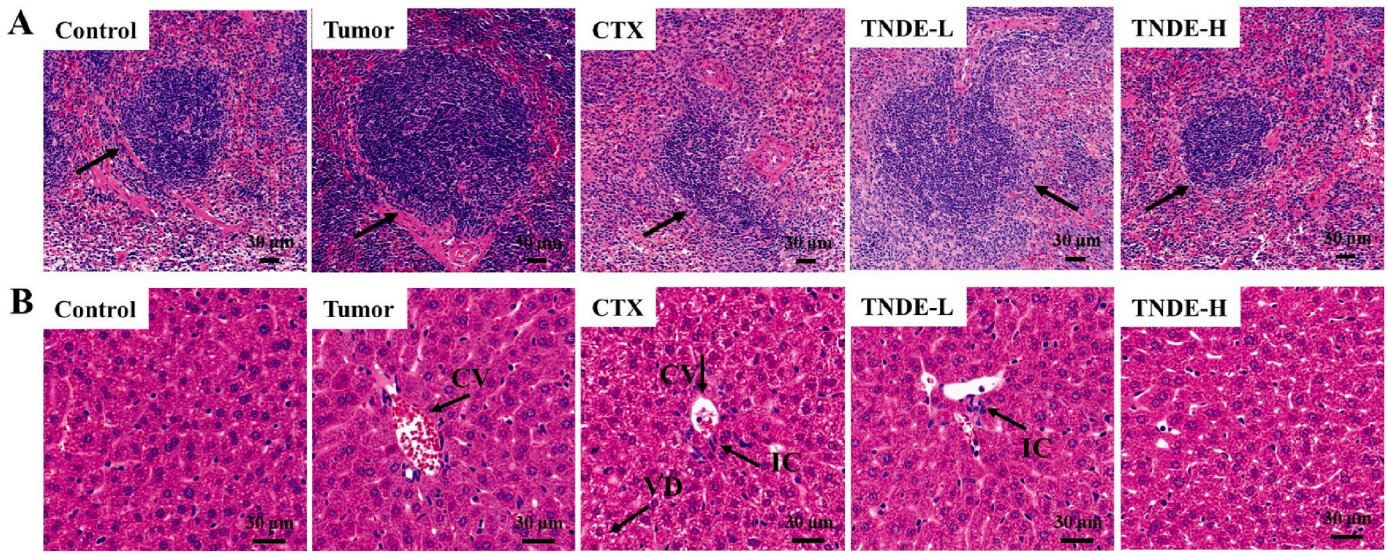

Fig. 4. Histopathological evaluation of the ameliorative effects of TNDE on spleen and liver in LLC mice undergoing CTX-chemotherapy (200× magnification). (A) Spleen tissue. Arrows represent splenic corpuscle. (B) Liver tissue. CV represent center veins, VD represent vacuolar degeneration, IC represent inflammatory cellular infiltration.

indicators of humoral immune function (Li et al., 2022). Collectively, TNDE may effectively mitigate chemotherapy-induced immunosuppression by maintaining immunoregulatory balance, inhibiting the production of pro-inflammatory factors, and enhancing immunoglobulin secretion.

3.2.4. *Effect of TNDE on hematologic parameters in LLC mice*

In clinical practice, hematologic parameters, including red blood cell (RBC) count, hemoglobin (HGB) levels, white blood cell (WBC) count, granulocyte (GRAN) percentage, and lymphocyte (LYM) percentage, are key indicators used to evaluate chemotherapy-associated cachexia (Zhang, Zhou, et al., 2021). Hematological analyses of mice were performed, with results summarized in Table 2. All hematologic parameters in the CTX group were notably reduced compared to those in the control and tumor groups ($P < 0.01$). Mice treated with TNDE exhibited a dose-dependent improvement in these parameters, though most changes did not reach statistical significance ($P > 0.05$). Notably, TNDE supplementation significantly increased RBC levels in chemotherapy-treated mice compared to the CTX group ($P < 0.05$). The observed improvement may be attributed to the critical role of RBCs in immunomodulatory responses, including maintaining tissue oxygenation, acid-base balance, metabolic support, macrophage interactions, and signal transmission (Gao et al., 2019). These findings suggest that oral nutritional supplements, such as TNDE, can mitigate the adverse effects of chemotherapy and synergistically enhance treatment outcomes by providing high-quality nutrients.

3.2.5. *Effect of TNDE on tissue in histopathological evaluation*

The condition of immune organs is considered a fundamental indicator of an organism's immune potential, and the spleen is a vital immunological organ (Martini et al., 2016). Chemotherapy-induced splenic injury results from CTX-induced immunomodulatory dysfunction. To assess the ameliorative effects of TNDE on chemotherapy-induced immunosuppression, the pathological morphology of mouse spleen tissue was examined using H&E staining (Fig. 4A). In normal mice, splenocytes are tightly arranged, splenic corpuscles are well-defined, red and white pulp boundaries are distinct, and marginal areas appear normal. LLC mice not receiving chemotherapy showed dysplasia of splenic corpuscles. In contrast, LLC mice treated with chemotherapy exhibited severe damage to splenic corpuscles, including extensive destruction of the periosteal structure, a significant reduction in lymphocyte numbers, blurred red and white pulp boundaries, and thickened marginal zones. Chemotherapy-induced damage to immune organs and inhibition of splenic lymphocyte proliferation resulted in a marked suppression of immune function (Xu et al., 2023). Increasing oral doses of TNDE gradually restored the germinal centers of chemotherapy-treated LLC mice to levels comparable to those in normal mice. Lymphocyte numbers significantly increased, red and white pulp boundaries became distinct, and splenocytes exhibited an orderly arrangement, resembling the splenic morphology of normal mice. These observations align with the previously reported spleen index results. Ovalbumin-digested peptides have been shown to mitigate CTX-induced splenic damage, enhancing immunological function (Shao, Li, Zhu, & Sun, 2024). These findings suggest that TNDE alleviates immunosuppression in mice by mitigating immune organ damage and regulating cytokine production.

In addition to splenic damage, chemotherapy commonly causes liver injury (Zhang et al., 2022). To evaluate the protective effects of TNDE, the pathological morphology of liver tissue was analyzed (Fig. 4B). In normal mice, liver tissue exhibited a clear structure, binucleated hepatocytes, uniform chromatin, and no signs of inflammatory cell infiltration. In the tumor group, central veins and hepatocyte arrangements appeared disorganized. Chemotherapy further exacerbated liver damage in LLC mice, evidenced by inflammatory cell infiltration, narrowed hepatic sinusoids, unclear cell boundaries, reduced binucleated cells, vacuolar degeneration of hepatocytes, and necrosis around the central veins of hepatic lobules. The liver plays a critical role in detoxifying foreign substances through biotransformation. When the toxic load exceeds the liver's capacity, cellular membranes become damaged, leading to hepatic dysfunction (Hong, Shen, Huang, Wu, & Xie, 2022). Oral administration of TNDE improved liver tissue structure, as evidenced by the gradual resolution of central venous necrosis and restoration of hepatocyte arrangement to a normal, orderly pattern. Hepatic sinusoids appeared clear and inflammatory cell infiltration was absent. These findings suggest that TNDE supplementation alleviates chemotherapy-induced hepatocellular injury, though the specific metabolic pathways involved require further investigation.

3.2.6. *Effect of TNDE on metabolism in LLC mice*

To investigate the regulatory mechanisms underlying the adjunctive nutritional support provided by TNDE, untargeted metabolomics analysis was performed on liver tissue samples. Group consistency and

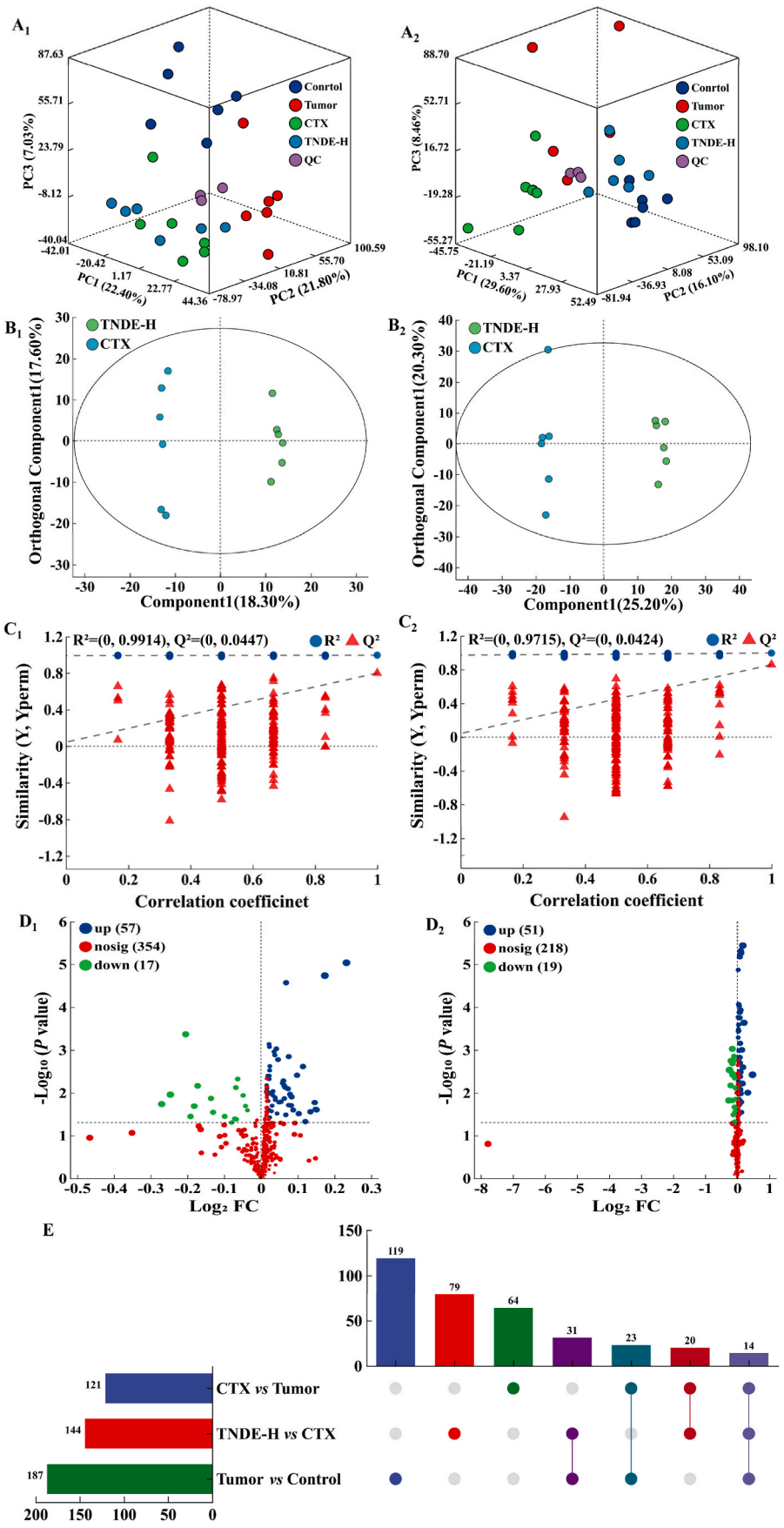

(caption on next page)

Fig. 5. Multivariate statistical analysis ($n = 6$). 3-Dimensional PCA score plot in positive ion mode (A_1) and negative ion mode (A_2). OPLS-DA score plot for the TNDE-H *vs* CTX in positive ion mode (B_1) and negative ion mode (B_2). OPLS-DA permutation plot for the TNDE-H *vs* CTX in positive ion mode (C_1) and negative ion mode (C_2). Volcanic plot for the TNDE-H *vs* CTX group in positive ion mode (D_1) and negative ion mode (D_2). Upset diagram showing the similarity and dissimilarity of differentially expressed metabolites in different groups (E).

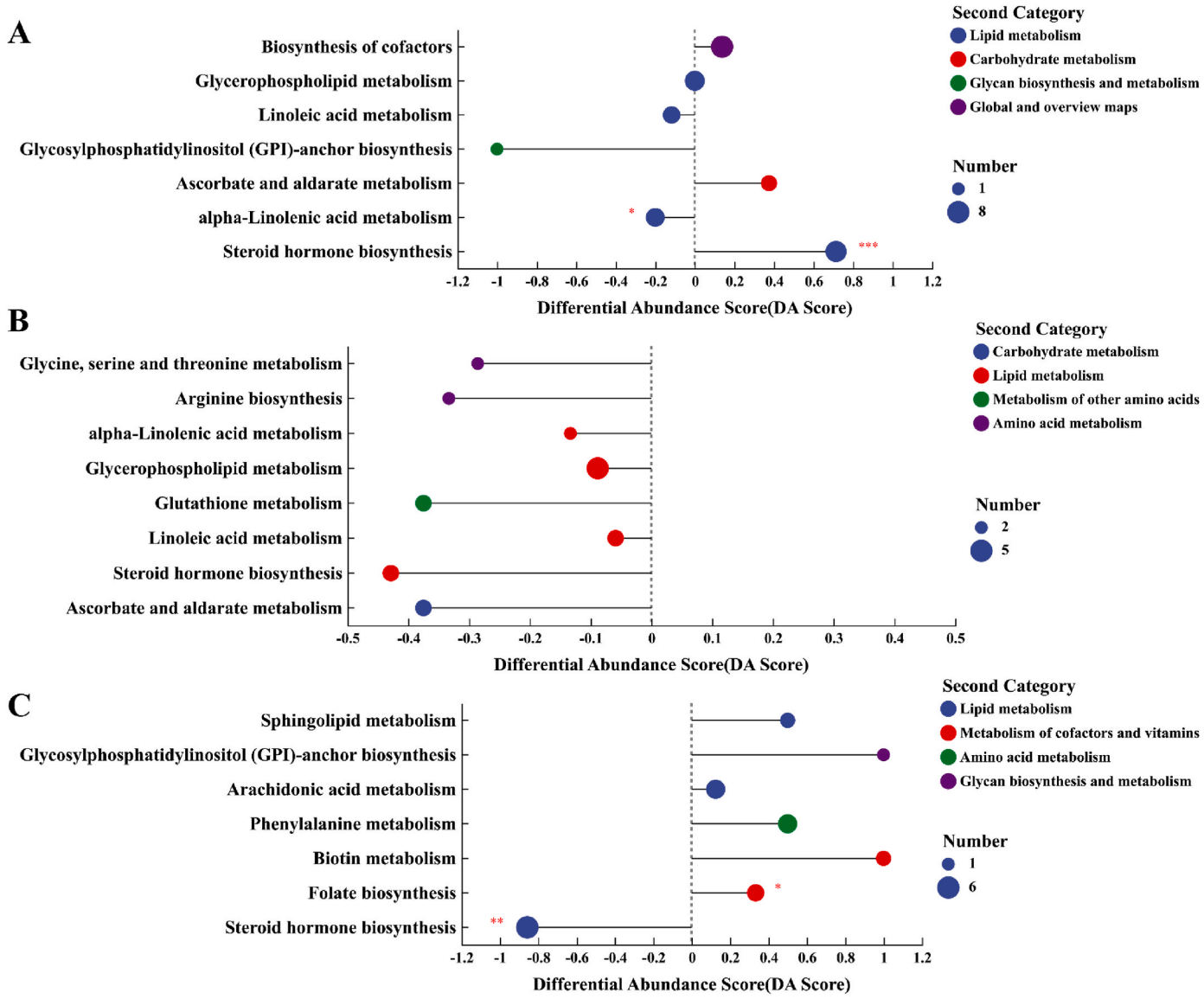

Fig. 6. Metabolic pathway analysis of the Tumor *vs* Control (A), CTX *vs* Tumor (B), and TNDE-H *vs* CTX (C) based on the differential abundance score. A score of 1 represents a trend of up-regulation of the expression of all annotated differential metabolites in the pathway, −1 represents a trend of down-regulation of the expression of all annotated differential metabolites in the pathway, and the length of the line segment indicates the absolute value of DA Score. The size of the dots indicates the number of annotated differential metabolites in the pathway, and a larger dot indicates a higher number of differential metabolites in the pathway.

differences were evaluated using three-dimensional principal component analysis (3D-PCA) and orthogonal partial least squares discriminant analysis (OPLS-DA) (Fig. 5A_1-B_2). Metabolic profiles differed significantly among the Control, Tumor, CTX, and TNDE-H groups, with clear separations observed in both positive and negative ion modes. These findings indicate that CTX chemotherapy substantially altered hepatic metabolism in mice. Additionally, the robustness of the OPLS-DA model was confirmed through 200 permutation tests ($R^2 > 0.97$), confirming strong reliability and the absence of overfitting (Fig. 5C_1 and C_2). A volcano plot, generated using VIP >1 and $P < 0.05$ as criteria, highlighted significant alterations in metabolite levels across groups in dual ion modes. Comparisons between the TNDE-H and CTX groups revealed 108 upregulated and 36 downregulated metabolites (Fig. 5D_1 and D_2), indicating substantial metabolic variations between these groups. An upset diagram was constructed to visually compare differentially expressed metabolites across groups (Fig. 5E). This analysis identified 121 unique metabolites in the CTX vs Tumor group, 144 unique metabolites in the TNDE-H vs CTX group, and 20 shared metabolites between the two comparisons.

Functional pathway analysis of the identified differential metabolites was conducted using the KEGG database to uncover key functional and metabolic pathways. Pathway classification indicated that amino acid and lipid metabolism pathways constituted the largest proportion (Fig. 6). The results showed that CTX chemotherapy significantly impacted several metabolic processes, including glycine, serine, and threonine metabolism, arginine biosynthesis, α-linolenic acid

metabolism, glycerophospholipid metabolism, glutathione metabolism, linoleic acid metabolism, steroid hormone biosynthesis, and ascorbate and aldarate metabolism in the CTX *vs* Tumor group. However, TNDE administration significantly up-regulated glycosylphosphatidylinositol-anchor biosynthesis, sphingolipid metabolism, arachidonic acid metabolism, phenylalanine metabolism, biotin metabolism, and folate biosynthesis. These findings align with a previous report by Zhang et al. (2024). Enrichment analysis further suggested that steroid hormone biosynthesis and folate biosynthesis are potential regulatory targets for TNDE in modulating hepatic metabolic pathways.

LLC mice exhibited enhanced cancer cell proliferation through significant upregulation of specific metabolic pathways. In contrast, CTX chemotherapy combined with oral TNDE effectively regulated these pathways, inhibiting tumor growth. Metabolites associated with metabolic disturbances, including 2-Hydroxyestradiol, Tetrahydrocortisone, 3α,11β,21-Trihydroxy-20-oxo-5β-pregnan-18-al, cortisol, cortolone, and dihydrocortisol, were significantly downregulated in chemotherapy-treated LLC mice following TNDE administration (Table S3). Steroid hormone biosynthesis, the pathway with the highest enrichment factors, was primarily influenced by the differential expression of cortisol. Aberrant expression of cell membrane transporter proteins has been implicated in lung cancer progression. The steroidogenic acute regulatory protein (StAR), a transmembrane transporter, facilitates cholesterol transfer from the outer to the inner mitochondrial membrane, a critical and rate-limiting step in cortisol synthesis (Tang et al., 2017). High expression levels of StAR have been associated with better prognostic outcomes (Cao et al., 2021). These findings suggest that the combination of CTX chemotherapy and oral TNDE inhibited cortisol production by upregulating steroidogenic acute regulatory proteins, thereby mitigating the malignancy associated with chemotherapy. Folate biosynthesis also emerged as a significantly regulated pathway following TNDE administration. Metabolites involved in this pathway, such as 7-Aminomethyl-7-carbaguanine and folic acid, were significantly upregulated. Folic acid is crucial for maintaining genomic stability by regulating DNA biosynthesis, repair, and methylation (Krupenko et al., 2019). The interconnected reactions of folate metabolism, known as single-carbon metabolism, include processes such as amino acid synthesis, nucleotide production, and breakdown (Tibbetts & Appling, 2010). TNDE positively modulated folate biosynthesis, balancing cellular energy and promoting metabolic stability. These findings suggest that TNDE mitigates chemotherapy-induced cachexia by restoring abnormal cellular energy metabolism and nutrient absorption while preserving chemotherapeutic efficacy.

4. Conclusion

The findings of this study demonstrate that TNDE is a nutritionally advantageous supplement enriched with BCAAs, hydrophobic amino acids, and ω-3 PUFAs. TNDE supplementation significantly alleviated immunosuppression, malnutrition, and other symptoms of cachexia in LLC mice undergoing CTX chemotherapy. Additionally, TNDE enhanced the therapeutic efficacy of CTX by downregulating steroid hormone biosynthesis and upregulating folate biosynthesis. These results suggest that TNDE holds potential as a functional emulsion for enteral nutritional intervention in oncology patients during treatment.

CRediT authorship contribution statement

Jinzhen Li: Writing – original draft, Visualization, Validation, Methodology, Investigation, Formal analysis, Data curation. **Wenhong Cao:** Validation, Investigation. **Zhongqin Chen:** Validation, Investigation. **Haisheng Lin:** Validation, Investigation. **Jialong Gao:** Validation, Investigation. **Mingtang Tan:** Validation, Investigation. **Xiaoming Qin:** Validation, Investigation. **Huina Zheng:** Writing – review & editing, Supervision, Project administration, Funding acquisition.

Declaration of competing interest

The authors declare that they have no known competing financial interests or personal relationships that could have appeared to influence the work reported in this paper.

Acknowledgment

This work was supported by the Guangdong Basic and Applied Basic Research Foundation (2024A1515010955), the Guangdong Province Modern Agricultural Industrial Technology System Innovation Team Construction Project (2024), the Modern Agricultural Industry Technology Research System of China (CARS-49), and the National Key R&D Program of China (2024YFD2401805).

Appendix A. Supplementary data

Supplementary data to this article can be found online at https://doi.org/10.1016/j.fbio.2025.105968.

Data availability

Data will be made available on request.

References

Alduais, Y., Zhang, H., Fan, F., Chen, J., & Chen, B. (2023). Non-small cell lung cancer (NSCLC): A review of risk factors, diagnosis, and treatment. *Medicine, 102*(8), Article e32899.

Augustin, K., Khabbush, A., Williams, S., Eaton, S., Orford, M., Cross, J., et al. (2018). Mechanisms of action for the medium-chain triglyceride ketogenic diet in neurological and metabolic disorders. *The Lancet Neurology, 17*(1), 84–93.

Bray, F., Laversanne, M., Sung, H., Ferlay, J., Siegel, R., Soerjomataram, I., et al. (2024). Global cancer statistics 2022: GLOBOCAN estimates of incidence and mortality worldwide for 36 cancers in 185 countries. *Ca-A Cancer Journal for Clinicians, 74*(3), 229–263.

Buyukkestelli, H., & El, S. (2019). Development and characterization of double emulsion to encapsulate iron. *Journal of Food Engineering, 263*, 446–453.

Buyukkestelli, H., & El, S. (2021). Enhancing sweetness using double emulsion technology to reduce sugar content in food formulations. *Innovative Food Science & Emerging Technologies, 74*, Article 102809.

Calder, P. C. (2015). Marine omega-3 fatty acids and inflammatory processes: Effects, mechanisms and clinical relevance. *Biochimica et Biophysica Acta, Molecular and Cell Biology of Lipids, 1851*(4), 469–484.

Cao, P., Wu, S., Guo, W., Zhang, Q., Gong, W., Li, Q., et al. (2021). Precise pathological classification of non-small cell lung adenocarcinoma and squamous carcinoma based on an integrated platform of targeted metabolome and lipidome. *Metabolomics, 17*(11), 98.

Cockbain, A., Toogood, G., & Hull, M. (2012). Omega-3 polyunsaturated fatty acids for the treatment and prevention of colorectal cancer. *Gut, 61*(1), 135–149.

Drapala, K., Mulvihill, D., & O'Mahony, J. (2018). A review of the analytical approaches used for studying the structure, interactions and stability of emulsions in nutritional beverage systems. *Food Structure-Netherlands, 16*, 27–42.

Freitas, R., & Campos, M. (2019). Protective effects of omega-3 fatty acids in cancer-related complications. *Nutrients, 11*(5), 945.

Gao, X., Qu, H., Gao, Z., Zeng, D., Wang, J., Baranenko, D., et al. (2019). Protective effects of *Ulva pertusa* polysaccharide and polysaccharide iron (III) complex on cyclophosphamide induced immunosuppression in mice. *International Journal of Biological Macromolecules, 133*, 911–919.

Godsland, I. (2010). Insulin resistance and hyperinsulinaemia in the development and progression of cancer. *Clinical Science, 118*(5), 315–332.

Hashemirad, F.-S., Behfar, M., & Kavoosi, G. (2024). Proximate composition, physicochemical, techno-functional, amino acid profile, fatty acid profile, nutritional quality, antioxidant, anti-amylase and anti-lipase properties of bee bread, royal jelly, and bee propolis. *Lebensmittel-Wissenschaft und -Technologie, 200*, Article 116190.

Hong, Y., Shen, M., Huang, L., Wu, T., & Xie, J. (2022). *Mesona chinensis* Benth polysaccharides alleviates liver injury by beneficial regulation of gut microbiota in cyclophosphamide-induced mice. *Food Science and Human Wellness, 11*(1), 74–84.

International, A. (2023). *Official methods of analysis of AOAC International* (22nd ed.). Gaithersburg: AOAC.

Krupenko, N., Sharma, J., Pediaditakis, P., Fekry, B., Helke, K., Du, X., et al. (2019). Cytosolic 10-formyltetrahydrofolate dehydrogenase regulates glycine metabolism in mouse liver. *Scientific Reports, 9*(1), Article 14937.

Kumar, A., Kaur, R., Kumar, V., Kumar, S., Gehlot, R., & Aggarwal, P. (2022). New insights into water-in-oil-in-water (W/O/W) double emulsions: Properties, fabrication, instability mechanism, and food applications. *Trends in Food Science & Technology, 128*, 22–37.

Lamba, H., Sathish, K., & Sabikhi, L. (2015). Double emulsions: Emerging delivery system for plant bioactives. *Food and Bioprocess Technology, 8*(4), 709–728.
Li, J., Chen, Y., Lin, H., Chen, Z., Cao, W., Gao, J., et al. (2024). Comparison of ultrasound and high-pressure homogenization emulsification: A promising fabrication strategy for total nutritional double emulsion-based product enriched with low-molecular-weight oyster peptides. *Lebensmittel-Wissenschaft und -Technologie, 212*, Article 116981.
Li, J., Wang, S., Wang, H., Cao, W., Lin, H., Qin, X., et al. (2023). Effect of ultrasonic power on the stability of low-molecular-weight oyster peptides functional-nutrition $W_1/O/W_2$ double emulsion. *Ultrasonics Sonochemistry, 92*, Article 106282.
Li, J., Yang, L., Li, G., Liu, S., Cao, W., Lin, H., et al. (2022). Low-molecular-weight oyster peptides ameliorate cyclophosphamide-chemotherapy side-effects in Lewis lung cancer mice by mitigating gut microbiota dysbiosis and immunosuppression. *Journal of Functional Foods, 95*, Article 105196.
Liu, Y., Chan, Y., Wu, T., Li, T., Hsia, S., Chiu, Y., et al. (2019). Antitumor, inhibition of metastasis and radiosensitizing effects of total nutrition formula on lewis tumor-bearing mice. *Nutrients, 11*(8), 1194.
Liu, Y., Chen, X., Yang, J., Guo, Z., Wu, Q., Zhang, L., et al. (2023). RNA-seq analysis reveals an immunomodulatory peptide from highland barley activating RAW264.7 macrophages via TNF/NF-κB signaling pathway. *Functional & Integrative Genomics, 23*(3), 253.
Liu, Y., Wu, T., Chiu, Y., Wang, H., Li, T., Hsia, S., et al. (2020). Positive effects of preventive nutrition supplement on anticancer radiotherapy in lung cancer bearing mice. *Cancers, 12*(9), 2445.
Martini, E., Wittkopf, N., Günther, C., Leppkes, M., Okada, H., Watson, A., et al. (2016). Loss of survivin in intestinal epithelial progenitor cells leads to mitotic catastrophe and breakdown of gut immune homeostasis. *Cell Reports, 14*(5), 1062–1073.
Mele, M., Rinninella, E., Cintoni, M., Pulcini, G., Di Donato, A., Grassi, F., et al. (2021). Nutritional support in lung cancer patients: The state of the art. *Clinical Lung Cancer, 22*(4), E584–E594.
Michel, M., Eldridge, A., Hartmann, C., Klassen, P., Ingram, J., & Meijer, G. (2024). Benefits and challenges of food processing in the context of food systems, value chains and sustainable development goals. *Trends in Food Science & Technology, 153*, Article 104703.
Mir, N., Riar, C., & Singh, S. (2019). Effect of pH and holding time on the characteristics of protein isolates from *Chenopodium* seeds and study of their amino acid profile and scoring. *Food Chemistry, 272*, 165–173.
Naudhani, M., Thakur, K., Ni, Z., Zhang, J., & Wei, Z. (2021). Formononetin reshapes the gut microbiota, prevents progression of obesity and improves host metabolism. *Food & Function, 12*(24), 12303–12324.
Nie, C., He, T., Zhang, W., Zhang, G., & Ma, X. (2018). Branched chain amino acids: Beyond nutrition metabolism. *International Journal of Molecular Sciences, 19*(4), 954.
Shao, Z., Li, X., Zhu, H., & Sun, H. (2024). Ovalbumin-digested peptides can reverse cyclophosphamide-induced immune dysfunction in mice. *Food Bioscience, 58*, Article 103642.
Tang, Z., Li, C., Kang, B., Gao, G., Li, C., & Zhang, Z. (2017). Gepia: A web server for cancer and normal gene expression profiling and interactive analyses. *Nucleic Acids Research, 45*(1), 98–102.
Tibbetts, A., & Appling, D. (2010). Compartmentalization of mammalian folate-mediated one-carbon metabolism. *Annual Review of Nutrition, 30*, 57–81.
Torricelli, P., Antonelli, F., Ferorelli, P., Borromeo, I., Shevchenko, A., Lenzi, S., et al. (2020). Oral nutritional supplement prevents weight loss and reduces side effects in patients in advanced lung cancer chemotherapy. *Amino Acids, 52*(3), 445–451.
Vinayashree, S., & Vasu, P. (2021). Biochemical, nutritional and functional properties of protein isolate and fractions from pumpkin (*Cucurbita moschata* var. Kashi Harit) seeds. *Food Chemistry, 340*, Article 128177.
Wang, H., Hsia, S., Wu, T., & Wu, C. (2021). Fish oil, se yeast, and micronutrient-enriched nutrition as adjuvant treatment during target therapy in a murine model of lung cancer. *Marine Drugs, 19*(5), 262.
Wang, D., Huang, X., Marnila, P., Hiidenhovi, J., Välimaa, A., Granato, D., et al. (2024). Baltic herring hydrolysates: Identification of peptides, in silico DPP-4 prediction, and their effects on an in vivo mice model of obesity. *Food Research International, 191*, Article 114696.
Wang, Y., Liao, M., Zhang, Y., Deng, F., Luo, J., Wang, N., et al. (2021). Artesunate protects immunosuppression mice induced by glucocorticoids via enhancing pro-inflammatory cytokines release and bacterial clearance. *European Journal of Pharmacology, 890*, Article 173630.
Windsor, A., Kanwar, S., Li, A., Barnes, E., Guthrie, J., Spark, J., et al. (1998). Compared with parenteral nutrition, enteral feeding attenuates the acute phase response and improves disease severity in acute pancreatitis. *Gut, 42*(3), 431–435.
Wu, Y., Luo, J., & Xu, B. (2024). Insights into the anticancer effects of galangal and galangin: A comprehensive review. *Phytomedicine, 135*, Article 156085.
Xiao, Y., Liu, P., Wei, J., Zhang, X., Guo, J., & Lin, Y. (2023). Recent progress in targeted therapy for non-small cell lung cancer. *Frontiers in Pharmacology, 14*, Article 1125547.
Xu, X., Shao, T., Meng, Y., Liu, C., Zhang, P., & Chen, K. (2023). Immunomodulatory mechanisms of an acidic polysaccharide from the fermented burdock residue by *Rhizopus nigricans* in RAW264.7 cells and cyclophosphamide-induced immunosuppressive mice. *International Journal of Biological Macromolecules, 252*, Article 126462.
Yang, L., Gao, Y., Gong, J., Wang, H., Farag, M., Simal-Gandara, J., et al. (2022). Myricetin ameliorated prediabetes via immunomodulation and gut microbiota interaction. *Food Frontiers, 3*(4), 749–772.
Yao, C., Sun, R., Yang, Y., Zhou, H., Meng, Z., Chi, R., et al. (2023). Accumulation of branched-chain amino acids reprograms glucose metabolism in $CD8^+$ T cells with enhanced effector function and anti-tumor response. *Cell Reports, 42*(3), Article 112186.
Ying, X., Gao, J., Lu, J., Ma, C., Lv, J., Adhikari, B., et al. (2021). Preparation and drying of water-in-oil-in-water (W/O/W) double emulsion to encapsulate soy peptides. *Food Research International, 141*, Article 110148.
Zepeda-Hernández, A., Garcia-Amezquita, L., Requena, T., & García-Cayuela, T. (2021). Probiotics, prebiotics, and synbiotics added to dairy products: Uses and applications to manage type 2 diabetes. *Food Research International, 142*, Article 110208.
Zhang, J., Gao, S., Li, H., Cao, M., Li, W., & Liu, X. (2021). Immunomodulatory effects of selenium-enriched peptides from soybean in cyclophosphamide-induced immunosuppressed mice. *Food Science and Nutrition, 9*(11), 6322–6334.
Zhang, Y., He, P., Pan, L., Lin, Z., Yang, J., Wu, H., et al. (2023). Immunomodulatory effect of earthworm protein autolysates on cyclophosphamide(CTX)-induced immunosuppressed mice. *Food Bioscience, 56*, Article 103297.
Zhang, H., Lu, Y., Zhang, Y., Dong, J., Jiang, S., & Tang, Y. (2024). DHA-enriched phosphatidylserine ameliorates cyclophosphamide-induced liver injury via regulating the gut-liver axis. *International Immunopharmacology, 140*, Article 112895.
Zhang, N., Tian, Y., Wang, Y., Fan, Y., Zhang, Y., Xing, X., et al. (2022). Ameliorative effect of Lactobacillus plantarum Lp2 against cyclophosphamide-induced liver injury in mice. *Food and Chemical Toxicology, 169*, Article 113433.
Zhang, J., Zhou, H., He, S., Zhang, X., Ling, Y., Li, X. Y., et al. (2021). The immunoenhancement effects of sea buckthorn pulp oil in cyclophosphamide-induced immunosuppressed mice. *Food & Function, 12*(17), 7954–7963.
Zhao, X., An, X., Yang, C., Sun, W., Ji, H., & Lian, F. (2023). The crucial role and mechanism of insulin resistance in metabolic disease. *Frontiers in Endocrinology, 14*, Article 1149239.